HETEROCYCLES, Vol. 106, No. 7, 2023, pp. 1133 - 1144. © 2023 The Japan Institute of Heterocyclic Chemistry
Received, 3rd April, 2023, Accepted, 11th May, 2023, Published online, 17th May, 2023
DOI: 10.3987/COM-23-14855

CONSTRUCTION OF SUPRAMOLECULAR FRAMEWORKS COMPRISED OF FULLY-SUBSTITUTED CYCLOPENTANOCUCURBIT[6]URIL AND TWO PHENOLIC ACIDS

Naqin Yang,[a] Yue Ma,[b] Jun Zheng,[a] Xinan Yang,[a] and Peihua Ma[a]*

[a] Key Laboratory of Macrocyclic and Supramolecular Chemistry of Guizhou Province, Guizhou University, Guiyang 550025, People's Republic of China.

[b] Guiyang College of Humanities and Science, Guiyang 550025, People's Republic of China.

* E-mail: phma@gzu.edu.cn

Abstract – In this paper, fully substituted cyclopentanocucurbit[6]uril ($CyP_6Q[6]$) and calcium ions were coordinated in the presence of cadmium chloride in hydrochloric acid solution, followed by the addition of *p*-hydroxybenzoic acid (**G1**) and 2,5-dihydroxybenzoic acid (**G2**) to construct two supramolecular frameworks, respectively. Their structures and interactions were characterized using single-crystal X-ray diffraction, X-ray powder diffraction. The results showed that calcium ions coordinate with the carbonyl-fringed portals of $CyP_6Q[6]$, **G1** and **G2** act on the outer surface of $CyP_6Q[6]$ via C-H···π interactions, and $[CdCl_4]^{2-}$ participates in ion-dipole interactions with $CyP_6Q[6]$ to form a framework structure consisting of pores and layers.

INTRODUCTION

Studies on supramolecular framework materials are important in the field of supramolecular chemistry, and generally have periodic pore and pipe structures. They have typical applications in ion recognition and separation,[1-4] gas selective adsorption,[5,6] molecular reactors,[7] catalysis and so on.[8] Cucurbit[*n*]urils (Q[*n*]s) are a new generation of supramolecular macrocyclic host compounds after crown ethers, cyclodextrins and calixarenes.[9,10] The host-guest interactions between the neutral electrostatic hydrophobic cavities in Q[*n*]s and organic guest molecules,[11-13] coordination between negative electrostatic portal carbonyls and metal ions,[14-16] and the outer surface interactions between the positive electrostatic outer surface and solitary pair electron neutral molecules or anions[17-19] have been utilized to construct novel structures with mesh and porous supermolecular frameworks. Due to the poor solubility of ordinary cucurbit[*n*]urils, it is difficult to study their properties, and consequently, a series of modified cucurbit[*n*]urils have emerged. Cyclopentyl-substituted cucurbit[*n*]urils are new type of modified Q[*n*]s.[20] Due to the cyclopentyl group, its port is strongly negatively charged, which is not only superior to ordinary Q[*n*]s in terms of solubility, but it has certain potential applications for the construction and properties of supramolecular frameworks.

Currently, supramolecular frameworks based on fully-substituted cyclopentanocucurbit[6]uril ($CyP_6Q[6]$) are common. The coordination of its two identical carbonyl-fringed portals with some base metal ions (Li^+ and Na^+),[21] base soil metal ions (Mg^{2+}, Ca^{2+}, Sr^{2+} and Ba^{2+}),[22] transition metal ions (Fe^{3+}, Co^{2+} and Ni^{2+})[23] and lanthanide cations (Ln^{3+}),[24] or the host-guest interaction of its rigid hydrophobic cavity and organic guest molecules,[25,26] have successfully been used to construct a series of supramolecular framework materials. Phenolic acid organic guest molecules instead of hydroquinone are often used as organic structure inducers in the construction of supramolecular self-assembly of cucurbit[*n*]urils.[27,28] A series of novel multi-dimensional and multi-level cucurbit[*n*]uril-based coordination polymers were successfully constructed by π···π stacking and C-H···π interaction with the outer surface of cucurbit[*n*]urils, which can be used to selectively adsorb volatile organic compounds and provide a chiral coordination polymer synthesis and resolution method. However, the quaternary system supramolecular framework constructed using $CyP_6Q[6]$ and metal ions, phenolic acid organic guest molecules and inorganic anions has not been previously reported. Therefore, $CyP_6Q[6]$ and calcium ions (Ca^{2+}) were coordinated under the induction of $[CdCl_4]^{2-}$ in 3 mol/L hydrochloric acid solution, and *p*-hydroxybenzoic acid (**G1**) and 2,5-dihydroxybenzoic acid (**G2**) added to construct two quaternary system supramolecular frameworks, respectively. The structures of $CyP_6Q[6]$, **G1** and **G2** are shown in **Figure 1**.

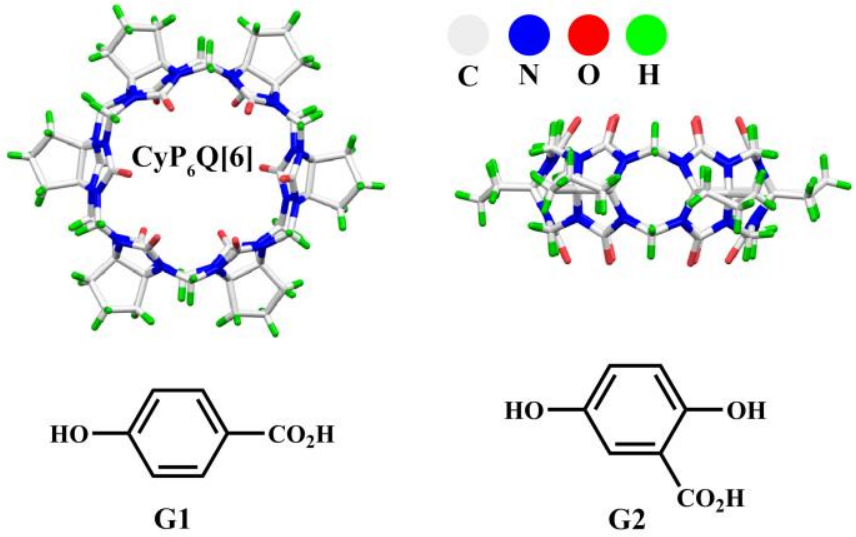

Figure 1. The structures of $CyP_6Q[6]$, *p*-hydroxybenzoic acid (**G1**) and 2,5-dihydroxybenzoic acid (**G2**)

RESULTS AND DISCUSSION

Description of crystal structure

The X-ray crystallographic data for structures reported in this study have been deposited at the Cambridge Crystallographic Data Centre under accession numbers CCDC: 2259482 (**Complex 1**) and 2164649 (**Complex 2**). These data can be obtained free of charge via http://www.ccdc.cam.ac.uk/data request/cif. The main crystal structure parameters are shown in **Table 1**.

Table 1. Crystallographic parameters of **complexes 1–2**

Complex	**1**	**2**
Empirical formula	$C_{150}H_{206}Ca_4Cd_4Cl_{16}N_{48}O_{68}$	$C_{68}H_{100}Ca_2Cd_2Cl_8N_{24}O_{34}$
Formula weight	4946.74	2386.27
Crystal system	Triclinic	Triclinic
Space group	*P*-1	*P*-1
a [Å]	10.3761(6)	10.400(2)
b [Å]	17.0226(9)	15.835(4)
c [Å]	28.5289(15)	16.540(4)

α [°]	90.200(2)	68.141(7)
β [°]	91.368(2)	84.184(7)
γ [°]	103.585(2)	71.450(7)
V [Å^3]	4896.4(5)	2396.1(9)
Z	1	1
$D_{calcd.}$ [g cm $^{-3}$]	1.678	1.654
T [K]	273.15	273.15
μ [mm $^{-1}$]	0.852	0.867
Parameters	1416	650
R_{int}	0.0372	0.0982
R[I > 2σ(I)][a]	0.0331	0.1217
wR[I > 2σ(I)][b]	0.0810	0.3271
R(all data)	0.0413	0.1548
wR(all data)	0.0860	0.3565
GOF on F^2	1.054	1.090
CCDC	2259482	2164649

[a]Conventional *R* on F*hkl*: $\sum||F_o| - |F_c||/\sum|F_o|$.

[b]Weighted R on |F*hkl*|^2: $\sum[w(F_o^2 - F_c^2)^2]/\sum[w(F_o^2)^2]^{1/2}$.

The crystal structure of **complex 1** ($C_{150}H_{206}Ca_4Cd_4Cl_{16}N_{48}O_{68}$) **(Figure 2**): From the crystal parameters (**Table 1**), the crystal structure was determined to be triclinic with a *P*-1 space group. The structural unit of the crystal shown in **Figure 2**, an asymmetric unit contains two $CyP_6Q[6]$ molecules, four Ca^{2+} ions, 18 coordinated water molecules, four free water molecules, two $[CdCl_4]^{2-}$ ions, and four **G1** molecules. The two Ca^{2+} ions coordinate with the carbonyl-fringed portals at one end of $CyP_6Q[6]$ and also directly

coordinate with the two **G1** molecules, which are cross-arranged due to steric hindrance. The other two Ca^{2+} ions coordinate with the carbonyl-fringed portals at both ends of $CyP_6Q[6]$, one Ca^{2+} ion on each side. In this system, hydrogen bonding is one of the main interactions, and $[CdCl_4]^{2-}$ anions form hydrogen bond with the coordinated water molecules (Cl1-O9W and Cl8-O2W) with bond lengths of 3.125 Å, and 3.070 Å, respectively. The hydroxyl group on the carboxyl group of **G1** was hydrogen-bonded with the coordinated water molecules and free water molecules (O14-O8W, O21-O22, and O18-O6W), and the distances between the two are 2.698, 2.755, and 2.630 Å, respectively. **Figure 2** shows that the coordinated water molecules interact with the carbonyl oxygen in $CyP_6Q[6]$ via hydrogen bonds ((O7-O10W, O12-O8W, O3-O5W, O6-O3W, O6-O1W) and bond lengths were in the range of 2.670 ~ 2.986 Å. Hydrogen bonds also occur between the coordinated water molecules on the two calcium ions (O10W-O11W) with a bond distance of 2.812 Å. **Figure 2d** shows the hydrogen bond interactions (O7W-O17, O7W-O13 and O7W-O4) between the free water molecules, **G1** and $CyP_6Q[6]$. The bond distances between them are 2.733, 2.629 and 2.723 Å, respectively. The free water molecules connect the **G1** molecules and $CyP_6Q[6]$ via hydrogen bonding interactions. Interestingly, the **G1** molecules around $CyP_6Q[6]$ not only interact via C-H···π interactions and C48-H···O19 with distances of 2.666 Å, but also directly coordinate with the Ca^{2+} ions, forming a novel structure. The purple curve in **Figure 2e** shows that $[CdCl_4]^{2-}$ participates in ion-dipole interactions (C-H···Cl interactions) with $CyP_6Q[6]$ and **G1** molecules. **Figure 3a** shows that two Ca^{2+} ions coordinate with the carbonyl oxygen atom of $CyP_6Q[6]$ molecules, **G1** molecules, and water molecules, form a polyhedral structure. Ca2-Owater distances are in the range of 2.353 ~ 2.512 Å, Ca2-O15 distance is 2.417 Å, and Ca2-Ocarbonyl distances are in the range of 2.377 ~ 2.518 Å. Ca^{2+} ions serve as a bridge between two $CyP_6Q[6]$ molecules, and the coordinated **G1** molecules are arranged in a crossover fashion on both sides of the molecular chain, forming a 1-D supramolecular chain. **Figure 3b** is the stacking diagram of the crystal structure of **complex 1** viewed along the a-axis. $[CdCl_4]^{2-}$ anions surround $CyP_6Q[6]$ molecules and form $[CdCl_4]^{2-}$-based honeycomb-like framework. **Figure 3d** shows the stacked diagram viewed along the b-axis, which shows two different 1-D supramolecular chains (yellow and red chains) of **complex 1**.

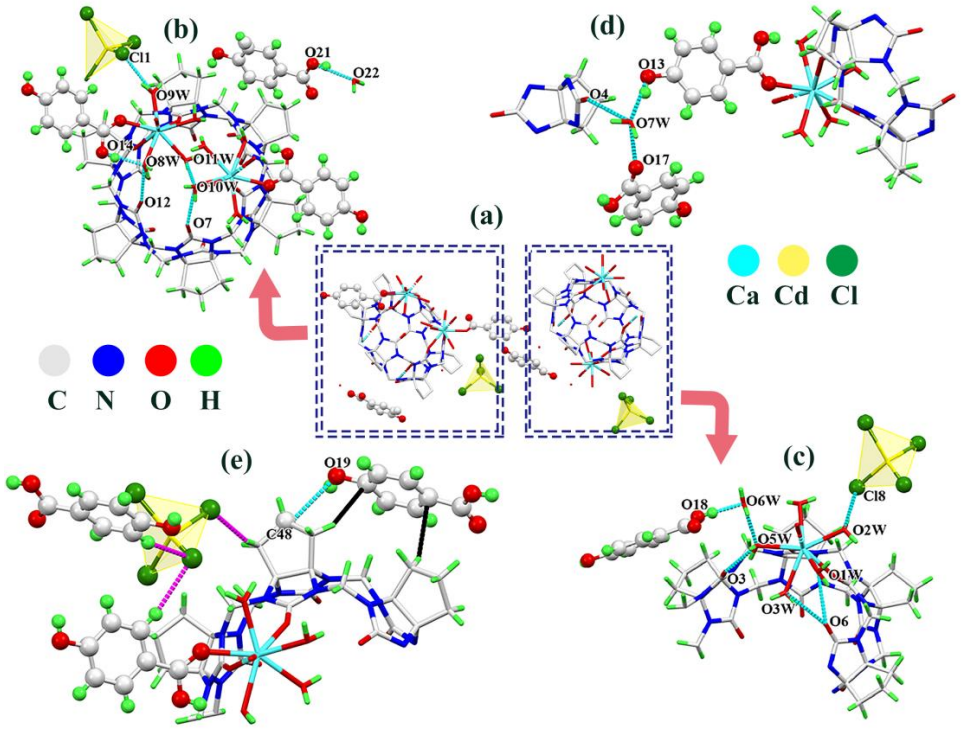

Figure 2. (a) Structural unit, (b, c, and d) hydrogen bond interactions, (e) C-H···π interactions and C-H···Cl interactions

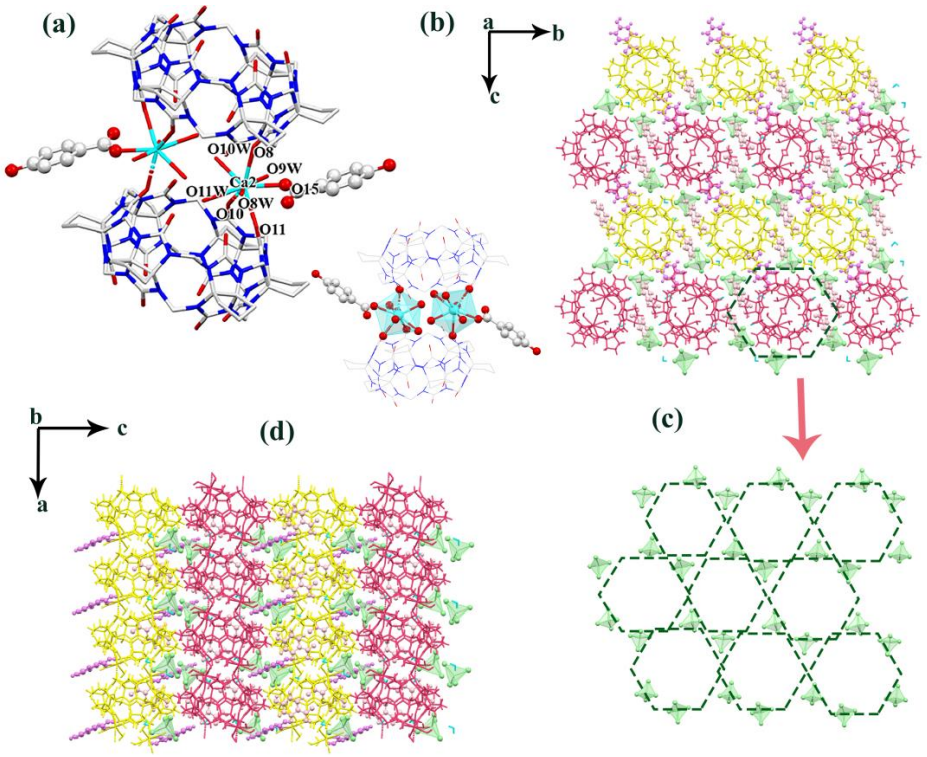

Figure 3. Detailed interactions of Ca^{2+} cations with $CyP_6Q[6]$ molecules, viewed along the (b) a-axis, (c) the $[CdCl_4]^{2-}$ -based honeycomb-like framework, (d) viewed along the b-axis

The crystal structure of **complex 2** ($C_{68}H_{100}Ca_2Cd_2Cl_8N_{24}O_{34}$) (**Figure 4**): An asymmetric unit of the crystal **(Figure 4a)** contains one $CyP_6Q[6]$ molecule, two calcium ions, ten coordinated water molecules, one $[CdCl_4]^{2-}$, two free water molecules, and one **G2** molecule. The two calcium ions simultaneously coordinate with the carbonyl-fringed portal at one end of $CyP_6Q[6]$. **Figure 4b** shows that the coordinated water molecule forms a hydrogen bond (O1W-O10) with the hydroxyl group on **G2** with a bond distance of 2.918 Å. At the same time, the coordinated water molecules interact with the carbonyl oxygen in $CyP_6Q[6]$ via hydrogen bonds (O3W-O4, O5W-O2) and bond lengths were 2.780, and 2.778 Å. The free water molecule forms hydrogen bond interactions with the hydroxyl group on the carboxyl group of the **G2** molecule and the carbonyl oxygen of $CyP_6Q[6]$ (O6W-O7 and O6W-O4), and the bond distances between the two are 2.599 and 2.781 Å, respectively. $[CdCl_4]^{2-}$ anion forms hydrogen bonds with the free water molecule (Cl3-O7W and Cl4-O7W) with bond lengths of 3.092 Å, and 3.005 Å, respectively. **G2** molecule has intramolecular hydrogen bond (O8-O9) with bond length 2.539 Å. As shown in **Figure 4c**, the **G2** molecules are located around $CyP_6Q[6]$ via C-H···π interactions and C3-H···O8 with distances of 2.600 Å. Ion-dipole interactions (C-H···Cl interactions) were formed between $[CdCl_4]^{2-}$ and $CyP_6Q[6]$. **Figure 4d** shows that every two neighbouring $CyP_6Q[6]$ molecules are linked by two Ca^{2+} cations, and each Ca^{2+} cation (Ca1) coordinates to eight oxygens, consisting of five water molecules (O1W, O2W, O3W, O4W, and O5W), and three portal carbonyl oxygens (O1, O6 from a $CyP_6Q[6]$ molecule, and O3 from another $CyP_6Q[6]$ molecule of the two neighbouring $CyP_6Q[6]$ molecules). Ca-Owater distances are in the range of 2.360 ~ 2.539 Å, and Ca-Ocarbonyl distances are in the range of 2.387 ~ 2.473 Å. Through direct coordination, Ca^{2+} cations play a bridging role in connecting two $CyP_6Q[6]$ molecules to form a 1-D supramolecular chain. **Figure 5a** shows the packing diagram of the crystal structure of **complex 2** viewed along the a-axis. $[CdCl_4]^{2-}$ anions surround $CyP_6Q[6]$ molecules and form a $[CdCl_4]^{2-}$-based honeycomb-like framework, with each cell in the framework filled with a $CyP_6Q[6]/Ca^{2+}$-based coordination polymer and **G2** molecule in which alternate $CyP_6Q[6]$ molecules and Ca^{2+} cations are linked through direct coordination. **Figure 5b** shows the stacked diagram viewed along the a*-axis. It can be clearly seen that **G2** molecules and $[CdCl_4]^{2-}$ are arranged in a row, and $CyP_6Q[6]/Ca^{2+}$-based coordination polymers are staggered, liking "sandwich biscuits".

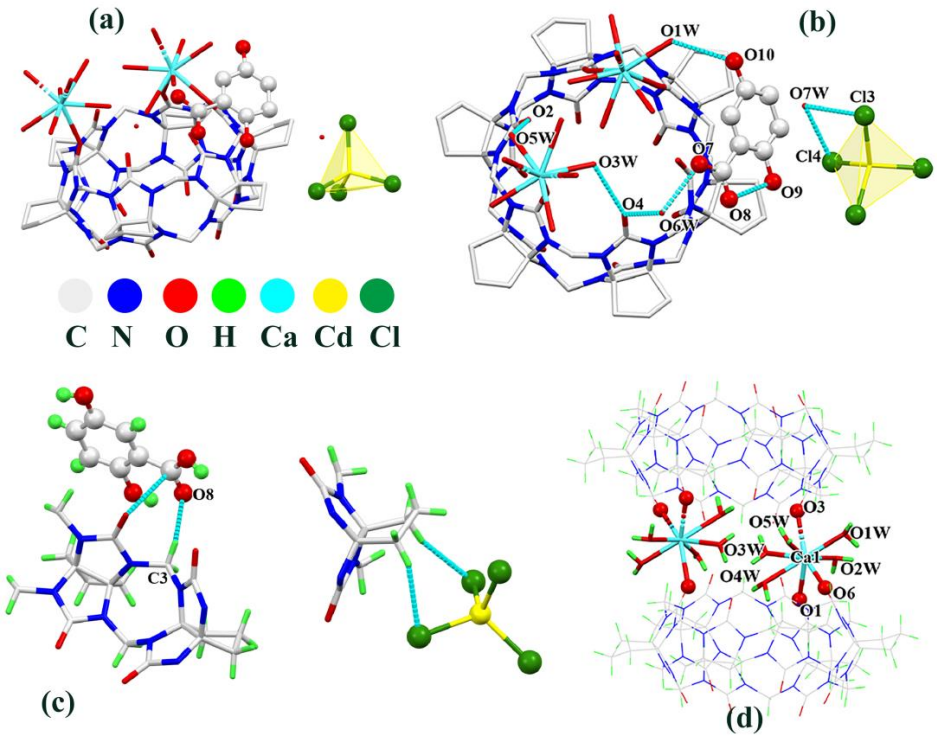

Figure 4. (a) Structural unit, (b) hydrogen bond interactions, (c) C-H···π interactions and ion-dipole interactions, (d) detailed interactions of Ca^{2+} cations with $CyP_6Q[6]$ molecules.

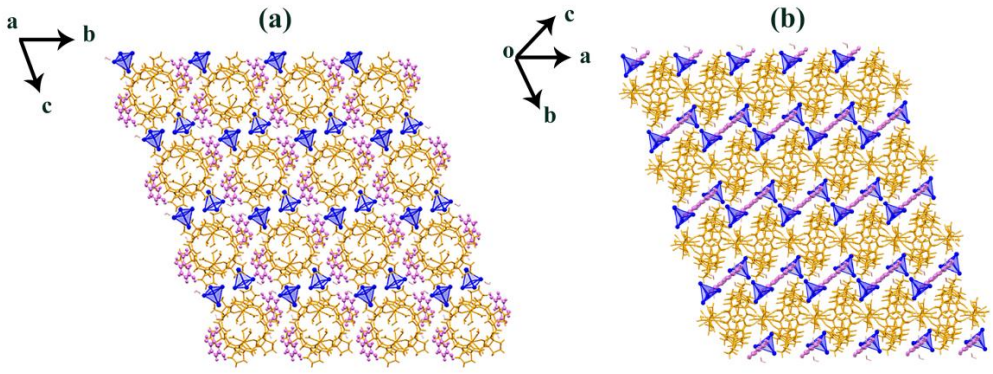

Figure 5. Structure stacking diagram viewed along the (a) a-axis, and (b) a*-axis

X-Ray powder difraction

The crystals of **complex 1** and **complex 2** were subjected to X-ray powder diffraction analysis. The X-ray powder diffraction spectrum of the sample and the crystalline material is basically matched in the angle, position of the diffraction peaks, which confirms that there are crystals of **complexes 1** and **2** in the powder, but the crystallinity is not very high. It can be further proved that **complexes 1** and **2** belong to the structure of heterogeneous isomorphism.

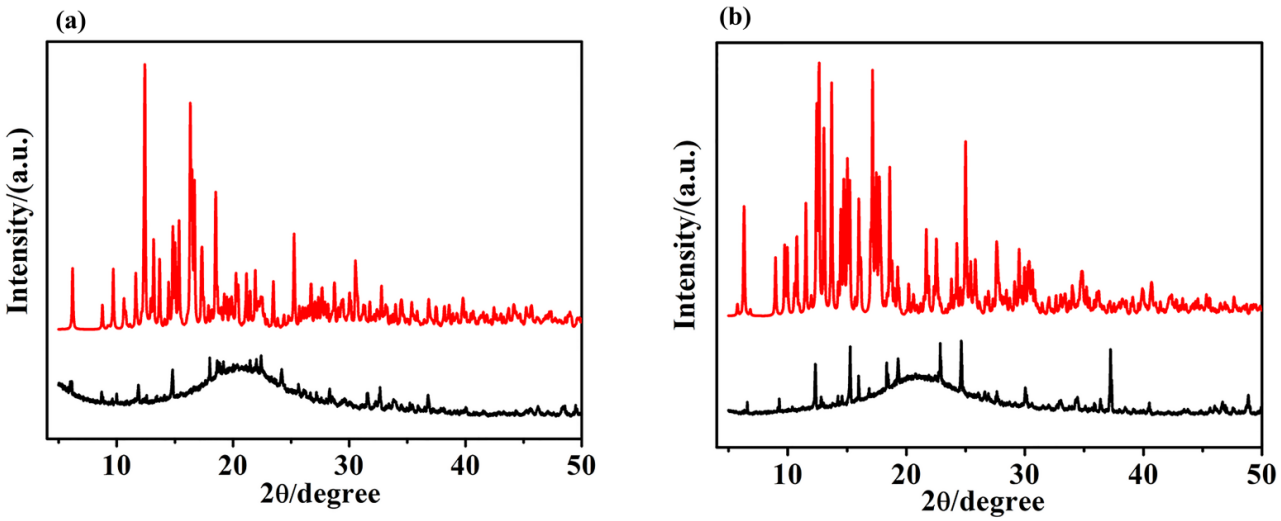

Figure 6. The actual X-ray powder diffraction results (Black line) and the theoretical X-ray powder diffraction results (Red line) of **complex 1** (a) and **complex 2** (b)

CONCLUSIONS

In summary, $CyP_6Q[6]$ and Ca^{2+} were coordinated under the induction of $[CdCl_4]^{2-}$ in hydrochloric acid solution, and **G1** and **G2** were added to construct two quaternary system supramolecular frameworks, respectively. The structures show that the two calcium ions coordinate with the negative electrostatic portal carbonyls of $CyP_6Q[6]$, **G1** and **G2** interact with the outer surface of $CyP_6Q[6]$ via C-H···π interactions, and $[CdCl_4]^{2-}$ participates in ion-dipole interactions with $CyP_6Q[6]$. The two novel supramolecular frameworks have obvious porous and layered structures, which are expected to have potential applications in the separation and purification of phenolic compounds and selective adsorption of volatile organic compounds.

EXPERIMENTAL

General Materials. All materials were reagent grade and used without any further purification. Fully substituted cyclopentanocucurbit[6]uril was prepared and purified in accordance to a previous method.[20]

Complex Preparation. Complex 1: $CyP_6Q[6]$ (15 mg, 12.1 μmol) was dissolved in hydrochloric acid solution (5 mL, 3 mol/L), and $CaCl_2$ (5.0 mg, 45.04 μmol) added and mixed evenly. $CdCl_2$ (6.0 mg, 32.72 μmol) and *p*-hydroxybenzoic acid (5.0 mg, 36.19 μmol) were then added to the mixture and heated under reflux for > 5 min. After cooling, the reaction mixture was filtered and the resulting solution was allowed to stand at room temperature for ~30 days. Crystals of $C_{150}H_{206}Ca_4Cd_4Cl_{16}N_{48}O_{68}$ suitable for single-crystal X-ray diffraction were formed. The yield was 36.8%.

Complex 2: $CyP_6Q[6]$ (15 mg, 12.1 μmol) was dissolved in hydrochloric acid solution (5 mL, 3 mol/L), and $CaCl_2$ (5.0 mg, 45.04 μmol) added and mixed evenly. $CdCl_2$ (4.0 mg, 21.82 μmol) and 2,5-dihydroxybenzoic acid (3.0 mg, 19.46 μmol) were then added to the mixture and heated under reflux for > 5 min. After cooling, the reaction mixture was filtered and the resulting solution was allowed to stand at room temperature for ~20 days. Crystals of $C_{68}H_{100}Ca_2Cd_2Cl_8N_{24}O_{34}$ suitable for single-crystal X-ray diffraction were formed. The yield was 40.6%.

X-Ray Crystallography. Determination of crystals entailed a method as previously described.[29] Diffraction data were collected on a Bruker Smart Apex II single-crystal X-ray diffractometer.

X-Ray Powder Diffraction. The X-ray powder difraction patterns were operated with a D8 advance small angle X-ray diffractometer using Cu-Kα radiation (k = 1.5418 Å, 60 kV, 60 mA), and the scanning rate was 5°/min. Powder samples were placed on a vitreous sample holder and scanned with a step size of 2θ = 0.02°, between 2θ = 5° and 90°.[30] The simulated powder diffraction pattern of the sample was derived from the Mercury software through the X-ray single crystal diffraction of the crystalline material and compared with the actual X-ray powder diffraction results.

ACKNOWLEDGEMENTS

This work was supported by the National Natural Science Foundation of China (Grant No.22161010).

REFERENCES

1. K. Chen, L. L. Liang, H. J. Liu, Y. Q. Zhang, S. F. Xue, Z. Tao, X. Xiao, Q. J. Zhu, L. F. Lindoy, and G. Wei, *CrystEngComm*, 2012, **14**, 7994.
2. X. D. Zhang, Y. Zhao, K. Chen, P. Wang, Y. S. Kang, H. Wuan, and W. Y. Sun, *Dalton Trans*., 2018, **47**, 3958.
3. D. Q. Zhang, Y. Q. Zhang, S. F. Xue, Z. Tao, X. Xiao, and Q. J. Zhu, *Polyhedron*, 2015, **99**, 147.
4. J. X. Liu, Y. F. Hu, R. L. Lin, W. Q. Sun, X. F. Chu, S. F. Xue, Q. J. Zhuan, and Z. Tao, *CrystEngComm*, 2012, **14**, 6983.
5. C. Z. Wang, W. X. Zhao, F. F. Shen, Y. Q. Zhang, Q. J. Zhu, X. Xiao, and Z. Tao, *CrystEngComm*, 2016, **18**, 2112.
6. Q. Li, S. C. Qiu, Y. Q. Zhang, S. F. Xue, Z. Tao, T. J. Prior, C. Redshaw, Q. J. Zhu, and X. Xiao, *RSC Adv.*, 2016, **6**, 77805.

7. Z. W. Gao, X. Feng, L. Mu, X. L. Ni, L. L. Liang, S. F. Xue, Z. Tao, X. Zeng, B. E. Chapman, P. W. Kuchel, L. F. Lindoy, and G. Wei, *Dalton Trans.*, 2013, **42**, 2608.
8. O. V. Nesterova, A. J. L. Pombeiro, and D. S. Nesterov, *Materials*, 2020, **13**, 5435.
9. J. Kim, I. S. Jung, S. Y. Kim, E. Lee, J. K. Kang, S. Sakamoto, K. Yamaguchi, and K. Kim, *J. Am. Chem. Soc.*, 2000, **122**, 540.
10. A. I. Day, R. J. Blanch, A. P. Arnold, S. Lorenzo, G. R. Lewis, and I. Dance, *Angew. Chem. Int. Ed.*, 2002, **41**, 275.
11. K. I. Assaf and W. M. Nau, *Chem. Soc. Rev.*, 2015, **44**, 394.
12. G. L. Hou, S. X. Min, Y. H. Zhao, B. Dong, L. N. Zhang, D. H. Li, W. C. Wu, H. F. Zhu, and B. Song, *Dyes Pigm.*, 2020, **180**, 108460.
13. D. E. Liu, X. J. Yan, J. X. An, J. B. Ma, and H. Gao, *J. Mater. Chem. B*, 2020, **8**, 7475.
14. O. A. Gerasko, M. N. Sokolov, and V. P. Fedin, *Pure Appl. Chem.*, 2004, **76**, 1633.
15. L. T. Wei, Y. Q. Zhang, K. Z. Zhou, L. L. Zhan, Y. X. Qu, Z. Tao, and P. H. Ma, *Inorg. Chim. Acta*, 2016, **453**, 277.
16. X. L. Ni, S. F. Xue, Z. Tao, Q. J. Zhua, L. F. Lindoy, and G. Wei, *Coordin. Chem. Rev.*, 2015, **287**, 89.
17. J. Zheng, W. W. Zhao, Y. Meng, Y. M. Jin, J. Gao, and P. H. Ma, *Cryst. Res. Technol.*, 2021, **56**, 2000183.
18. Y. Huang, R. H. Gao, M. Liu, L. X. Chen, X. L. Ni, X. Xiao, H. Cong, Q. J. Zhu, K. Chen, and Z. Tao, *Angew. Chem. Int. Ed.*, 2021, **60**, 15166.
19. R. H. Gao, Y. Huang, K. Chen, and Z. Tao, *Coord.. Chem. Rev.*, 2021, **437**, 213741.
20. F. Wu, L. H. Wu, X. Xiao, Y. Q. Zhang, S. F. Xue, Z. Tao, and A. I. Day, *J. Org. Chem.*, 2012, **77**, 606.
21. Y. M. Jin, S. Y. Cheng, T. H. Huang, W. W. Zhao, D. F. Jiang, J. Gao, X. N. Yang, and P. H. Ma, *Crystallogr. Rep.*, 2021, **66**, 1268.
22. Y. X. Qu, Y. Q. Zhang, K. Z. Zhou, L. T. Wei, L. L. Zhan, S. Y. Cheng, Z. Tao, and P. H. Ma, *ChemistrySelect*, 2017, **2**, 4360.
23. J. Zheng, Y. Ma, X. N. Yang, and P. H. Ma, *RSC Adv.*, 2022, **12**, 18736.
24. Y. X. Qu, K. Z. Zhou, K. Chen, Y. Q. Zhang, X. Xiao, Q. D. Zhou, Z. Tao, P. H. Ma, and G. Wei, *Inorg. Chem.*, 2018, **57**, 7412.
25. Y. M. Jin, T. H. Huang, W. W. Zhao, X. N. Yang, Y. Meng, and P. H. Ma, *RSC Adv.*, 2020, **10**, 37369.

26. S. Y. Cheng, W. W. Zhao, X. N. Yang, Y. Meng, L. T. Wei, Z. Tao, and P. H. Ma, *R. Soc. Open Sci.*, 2021, **8**, 202120.
27. X. Feng, K. Chen, Y. Q. Zhang, S. F. Xue, Q. J. Zhu, Z. Tao, and A. I. Day, *CrystEngComm*, 2011, **13**, 5049.
28. K. Chen, L. L. Liang, H. J. Liu, Z. Tao, S. F. Xue, Y. Q. Zhang, and Q. J. Zhu, *CrystEngComm*, 2012, **14**, 8049.
29. Y. M. Jin, Y. Meng, X. N. Yang, C. Zhu, Z. Tao, J. X. Liu, and P. H. Ma, *Cryst. Growth Des.*, 2021, **21**, 2977.
30. J. L. Lin, L. Yang, X. L. Liao, C. Z. Gao, and B. Yang, *J. Incl. Phenom. Macrocycl. Chem.*, 2019, **95**, 159.